

# Strategic Data Re-Uploads: A Pathway to Improved Quantum Classification Data Re-Uploading Strategies for Improved Quantum Classifier Performance

S. Aminpour<sup>1,2</sup>, Y. Banad<sup>1</sup>, and S. Sharif<sup>1,2</sup>, Member, IEEE

<sup>1</sup>School of Electrical and Computer Engineering, University of Oklahoma, Norman, OK 73019 USA

<sup>2</sup>Center for Quantum and Technology, University of Oklahoma, Norman, OK 73019 USA

Corresponding author: Sarah Sharif (email: s.sh@ou.edu).

**ABSTRACT** Quantum machine learning (QML) is a promising field that explores the applications of quantum computing to machine learning tasks. A significant hurdle in the advancement of quantum machine learning lies in the development of efficient and resilient quantum classifiers capable of accurately mapping input data to specific, discrete target outputs. In this paper, we propose a novel approach to improve quantum classifier performance by using a data re-uploading strategy. Re-uploading classical information into quantum states multiple times can enhance the accuracy of quantum classifiers. We investigate the effects of different cost functions, such as fidelity and trace distance, on the optimization process and the classification results. We demonstrate our approach to two classification patterns: a linear classification pattern (LCP) and a non-linear classification pattern (NLCP). We evaluate the efficacy of our approach by benchmarking it against four distinct optimization techniques: L-BFGS-B, COBYLA, Nelder-Mead, and SLSQP. Additionally, we study the different impacts of fixed datasets and random datasets. Our results show that our approach can achieve high classification accuracy and robustness and outperform the existing quantum classifier models.

**INDEX TERMS** Data Re-uploading, Fidelity, Linear and Non-linear Classification Pattern, Quantum Classifiers, Quantum Machine Learning, Trace Distance

## I. INTRODUCTION

Quantum computing (QC) leverages the principles of quantum mechanics, specifically entanglement, superposition, and interference, to execute computations [2]. Rooted in the foundational concepts of quantum theory, this field explores the intricacies of quantum information. Unlike classical information, which can be easily cloned, quantum information is subject to the no-cloning theorem, restricting its processing possibilities. However, quantum information processing offers advantages in communication and computational tasks, such as solving algebraic problems, reducing sample complexity, and enhancing optimization processes. Notably, even simplified models of quantum computation can solve complex tasks, thereby holding promise for advancements in machine learning and artificial intelligence [3].

Quantum machine learning represents a burgeoning intersection of disciplines that has garnered substantial interest [3-6]. At the heart of contemporary QML practices

is the training of quantum circuits, aimed at processing both classical and quantum [7-13].

The cross-pollination of ideas between quantum information processing and fields like artificial intelligence and machine learning is unlocking novel potentials [3]. While the complete spectrum of potential applications for QML is yet to be fully explored, it is reasonable to anticipate its transformative impact across various sectors, including cybersecurity [14, 15], meteorology [16], healthcare [17], finance [18], and agriculture [19]. This potential breadth of application is illustrated in figure 1, suggesting a vast horizon for quantum machine learning's contribution to modern challenges [2, 20]. Multilayered perceptron, also known as neural networks, has become a cornerstone of machine learning due to their versatile and powerful architecture [21]. In the emerging field of QML, quantum neural networks (QNNs) adapt this concept by leveraging quantum mechanics to process information [22].

These networks undergo a training process akin to their classical counterparts, where data is input into the quantum system, a cost function is computed based on the output, and the parameters of the QNN are iteratively adjusted through classical optimization techniques to minimize this cost function [21].

In supervised learning, classification stands out as a commonly used task, where input data ( $x$ ) is mapped to



**FIGURE 1.** Quantum machines make the bridge between quantum computing and machine learning for a world of possibilities, including but not limited to cybersecurity, weather, healthcare, finance, and agriculture.

discrete target outputs  $y$  through a function approximation, denoted as  $y = f(x)$ . The aim here is to develop a model that can predict the output with high accuracy for given inputs [23]. Classification tasks are broadly categorized into two types: binary classification, which involves distinguishing between two possible outcomes such as diagnosing cancer (positive or negative) or detecting email spam (spam or not spam); and multi-class classification, which involves categorizing inputs into more than two distinct classes, like identifying the subject of a photograph or recognizing digits in an image [24].

Binary classification, in particular, has been a focus of machine learning research due to its wide applicability and foundational nature. Quantum computing has introduced novel approaches to this problem, such as quantum similarity-based binary classifiers and kernel methods that utilize quantum interference and explore the quantum Hilbert space. These quantum-enhanced methods promise significant advancements in machine learning, offering new ways to harness the computational power of quantum systems for complex classification tasks [25, 26].

A significant area of focus within the QML domain is the development and refinement of quantum classifiers, which are quantum devices designed to solve classification problems in machine learning [27, 28]. Quantum classifiers have garnered considerable attention due to their potential to outperform classical classifiers in certain scenarios [27]. These classifiers leverage the principles of quantum superposition and entanglement to process and classify data in ways that are fundamentally different from their classical

counterparts [27, 28]. Numerous quantum classification techniques have been introduced, expanding the range of potential applications in quantum computing. These encompass quantum support vector machines [29], quantum kernel approaches [30, 31], quantum decision trees [32], quantum nearest neighbor methods [33], and classifiers based on quantum annealing [27]. Each algorithm offers a unique approach to harnessing quantum computational advantages for solving complex classification problems.

A notable breakthrough in the QML field is the concept of data re-uploading. This methodology involves the cyclic encoding of classical information into a quantum system, allowing for the repeated integration of diverse datasets into the quantum processing workflow. Data re-uploading enables the construction of universal quantum classifiers [1], where a quantum circuit is meticulously organized into a series of stages dedicated to data integration and single-qubit operations [34]. This approach not only enhances the flexibility and adaptability of quantum classifiers but also significantly boosts their accuracy and efficiency in handling various classification tasks.

Several studies have explored various optimization techniques to enhance the performance of quantum classifiers. Lockwood [35] presents a comprehensive empirical review of optimization techniques for quantum variational circuits, comparing 46 optimizer setups, including minimization methods such as L-BFGS-B, Nelder-Mead, and SLSQP, across different QML problems. Similarly, Lee et al. [36] propose an iterative layerwise optimization strategy for the quantum approximate optimization algorithm to reduce optimization costs while maintaining high approximation ratios. Their numerical simulations compare the performance of L-BFGS-B and Nelder-Mead optimizers in conjunction with the proposed strategy on the Max-cut problem. Although these studies provide valuable insights, there is still a lack of research comparing different minimization methods in combination with data reuploading techniques. The impact of data reuploading on the performance of various minimization methods remains largely unexplored. Further investigation into the interplay between data reuploading and different optimization techniques could potentially lead to more efficient and effective QML algorithms. Besides, while previous studies have investigated the effects of data reuploading on QML algorithms, there is a lack of research focusing on random datasets that mirror real-world scenarios [37]. By evaluating the performance of QML algorithms on random datasets that closely resemble actual data, we can gain valuable insights into their robustness and generalization capabilities, ultimately leading to the development of more efficient and reliable QML techniques. Our preliminary findings suggest that the proposed methodology demonstrates potential when applied to a randomized dataset, warranting further investigation to validate its efficacy and generalizability [38]. In addition,

we propose investigating an alternative cost function to further assess the performance and robustness of the classifier [39]. Specifically, we suggest employing the trace distance cost function to gain deeper insights into the classifier's behavior. By examining the classifier's response to this distinct cost function, we aim to better understand its adaptability and potential for generalization across different optimization criteria. This exploration will provide valuable information regarding the classifier's versatility and its ability to maintain effectiveness under varying conditions.

This research focuses on performing a comprehensive comparative evaluation of two different cost functions including fidelity and trace distance cost function and four distinct optimization techniques including L-BFGS-B, COBYLA, Nelder-Mead, and SLSQP methods, applied to a single-qubit classifier. Our exploration delves into two contrasting types of datasets: one that remains constant and another that embodies randomness. Furthermore, we explore two specific classification challenges—linear and non-linear patterns—to conduct a comprehensive comparison that encompasses all pertinent aspects. This approach allows us to explore the details of these problems and gain deeper insights into their inherent properties and nuances.

The structure of the paper unfolds as follows: Section 2 is dedicated to a comprehensive review of the relevant literature. Here, we introduce and compare different cost functions applicable to the quantum classifier, setting the stage for a nuanced understanding of their impacts and implications. Moving to Section 3, we elucidate the concept of a single-qubit quantum classifier, demonstrating its capability as a universal approximator for any given classification function. This section underscores the versatility and potential of single-qubit systems in QML. In section 4, we navigate through the intricacies of four different minimization methods tailored for the quantum classifier. This comparative analysis aims to shed light on the effectiveness and efficiency of each method, contributing to a deeper comprehension of their operational dynamics and suitability for specific tasks. Section 5 analyzes the performance of single-qubit classifiers across various linear and non-linear classification tasks, such as circle and line patterns. The paper demonstrates the practical applicability and adaptability of data re-uploading techniques in QML, employing diverse cost functions and minimization strategies.

## II. QUANTUM CLASSIFIER

Quantum computing manipulates quantum systems to enhance information processing, leveraging superposition to simultaneously operate on multiple states for faster and more complex computation. At its core is the qubit, represented in a two-dimensional Hilbert space, with operations governed by quantum gates. These gates, essential for altering quantum states, must be unitary to ensure the conservation of

probability, a fundamental principle of quantum dynamics [5].

The framework of a quantum circuit unfolds in three key phases: encoding classical data into quantum format, manipulating the quantum state using quantum gates, and measuring the quantum state post-transformation. This process transitions from preparing an initial quantum state, through strategic alterations via quantum gates affecting computation outcomes, to a final probabilistic measurement—distinguishing quantum computing's potential and challenges from deterministic classical computing.

Achieving optimal performance in quantum computing requires a nuanced understanding of these phases, including the initial state preparation, the strategic selection and application of quantum gates, and the final measurement process. Each component must be meticulously optimized to perform specific tasks, such as classification, highlighting the intricate interplay between quantum mechanics and computational logic in the design and execution of quantum algorithms.

### A. RE-UPLOADING CLASSICAL INFORMATION AND PROCESSING

The integration of classical information into quantum computing represents a groundbreaking approach to data processing and analysis. This process begins with the strategic encoding of data into the initial wave function's coefficients within a quantum circuit [40]. In simpler terms, data is initially uploaded through the manipulation of qubits via rotational operations on a computational basis. This foundational step sets the stage for executing sophisticated quantum algorithms, including those designed for classification tasks.

The most successful programming paradigm in machine learning is predicated on artificial neural networks, which represent a highly abstracted and simplified model inspired by the human brain [41]. An artificial neural network comprises interconnected units or nodes known as artificial neurons, often arranged in layers [27]. These networks are characterized by their diverse architectures and the ability to learn from data through the adjustment of a vast network of parameters during the training phase. Among the various types of neural networks, feed-forward neural networks exemplify the process of sequential data processing, where input data is transformed layer by layer, simulating a form of data re-uploading at each neuron. This mechanism of data re-uploading and processing in ANNs provides a parallel to the innovative approach of constructing a universal quantum classifier using a single qubit. The essence of this quantum computing strategy lies in the repeated introduction of classical data at different stages of computation, analogous to the data processing in a single hidden layer neural network. This process can be visualized diagrammatically, as shown in figure 2. In figure 2(a), the neural network architecture is depicted, where data points are fed into individual processing

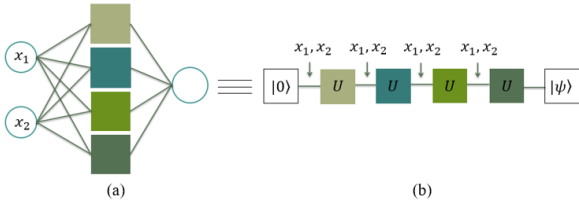


**FIGURE 2.** Comparison of the architectures between a neural network and a single-qubit quantum classifier with data re-uploading. (a) Depicts the structure of a classical neural network, where neurons in each layer receive and integrate inputs from all neurons in the previous layer. Conversely, (b) illustrates an architecture for a quantum classifier using a single qubit and data re-uploading. In this setup, the qubit's state is determined not only by the preceding processing units but also by classical input data that is repeatedly introduced. The output is a quantum state that encodes the cumulative effects of multiple rounds of data uploading and quantum processing steps.

units, analogous to neurons within the hidden layer. These neurons collectively process these input data, culminating in the activation of a final neuron responsible for constructing the output for subsequent analysis. Similarly, in the quantum domain, the single-qubit classifier incorporates data points into each stage of the computation through unitary rotations. These rotations are not isolated; rather, each one builds upon the transformations applied by its predecessors, effectively integrating the input data multiple times throughout the computation. The culmination of this process is a quantum state that encapsulates the computational outcome.

To construct a universal quantum classifier with only a single qubit, a complex integration of data input and computational processing within a single quantum circuit is crucial. We achieve this objective through the deployment of parametrized quantum circuits (PQCs). In these circuits, certain rotational angles are meticulously adjusted based on classical parameters, which are refined through an optimization process aimed at minimizing a specifically defined cost function.

The cost function plays a pivotal role in the operational efficacy of the quantum classifier. It quantitatively assesses the circuit's performance in segregating data points into distinct categories, which are represented as separate regions on the Bloch sphere. Each of these regions corresponds to a different class, and the classifier's goal is to assign data points to the correct class based on their features.

## B. MEASUREMENT

In the realm of quantum computing, a quantum circuit is distinguished by its processing angles  $\theta_i$  and associated weights  $w_j$ , leading to the generation of a final state  $|\mu\rangle$ . The measurement outcomes from this state are used to compute a classification error metric, defined as  $\chi^2$ . The goal is to minimize this error metric by adjusting the circuit's classical parameters, a process that can be effectively managed through various supervised machine learning techniques.

At the heart of using quantum measurement for classification tasks lies the approach of optimally aligning

observed outputs with specific target classes. This alignment is primarily facilitated by the principle of maximizing orthogonality between the output states, ensuring clear distinction [42]. In the context of binary (dichotomous) classification, this means categorizing each observation into one of two predefined classes—referred to here as Class A and Class B. The decision criterion involves comparing the probabilities of observing the quantum state  $P(0)$  for outcome 0 and  $P(1)$  for outcome 1. If  $P(0) > P(1)$ , the observation is assigned to class A; otherwise, it falls under class B. To enhance this binary classification scheme, one can introduce a bias ( $\lambda$ ), adjusting the threshold for classification such that observation is deemed part of Class A if  $P(0)$  is greater than  $\lambda$ , and Class B if it falls below. The value of  $\lambda$  is chosen to maximize classification accuracy on a training dataset. The effectiveness of this approach is then confirmed through evaluation on a separate validation dataset.

Enhanced classification accuracy is realized by determining the overlap between the final quantum state and a collection of predefined label states, specifically selected for their pronounced orthogonality. This technique aims to identify points of maximal orthogonality within the Bloch sphere, thereby facilitating classification. This approach is adept at accommodating both linear and nonlinear classification patterns, as depicted in the illustrative figure 3. Figure 3(a) demonstrates the geometric representation of two target states within the Bloch sphere, showcasing the assignment of data points to maximally orthogonal target states for precise classification. Figure 3(b) depicts the classification of data points into two distinct classes. In figure 3(c), a Non-Linear Classification Problem (NLCP) is presented. Here, data points are classified as either inside or outside a circle, with each classification corresponding to a different target state. Finally, figure 3(d) demonstrates a Linear Classification Problem (LCP). In this scenario, data points are classified as either above or below a line, again each classification corresponds to a unique target state.

Viewed through a geometric lens, the single-qubit classifier operates within a 2-dimensional Hilbert space—the Bloch sphere—where data encoding and classification decisions are delineated through specific rotational parameters. Any operation  $L(i)$  is a rotation on the Bloch sphere surface. From this viewpoint, any point can be classified using just one unitary operation. Consequently, we can transfer any point to another point on the Bloch sphere by precisely selecting the rotation angles. However, when dealing with multiple data points, a single rotation may not suffice due to differing optimal rotation requirements. The solution lies in introducing additional layers into the quantum circuit, enabling distinct rotation and fostering a richer feature map. Within this enhanced feature space, data points can be effectively segregated into their respective classes based on their positioning within the Bloch sphere's regions,

thereby enabling a sophisticated and adaptable approach to quantum classification.

### 1) FIDELITY COST FUNCTION

The goal is to align the quantum states  $|\psi(\vec{\theta}, \vec{w}, \vec{x})\rangle$  as closely as possible to a designated target state on the Bloch sphere, as outlined in [1]. This alignment can be quantitatively assessed by measuring the angular distance between the labeled state and the data state, using the metric of relative fidelity [43]. The primary objective focuses on maximizing the average fidelity between the quantum states produced by the circuit and the label states corresponding to their respective classes. To facilitate this, a cost function is introduced and mathematically formulated as Equation 1:

$$\chi_f^2(\vec{\theta}, \vec{w}) = \sum_{\mu=1}^M \left( 1 - \left| \langle \tilde{\psi}_s | \psi(\vec{\theta}, \vec{w}, \vec{x}_\mu) \rangle \right|^2 \right) \quad (1)$$

where  $|\tilde{\psi}_s\rangle$  is the correct label state of the  $\mu$  data point, which will correspond to one of the classes.

### 2) TRACE DISTANCE COST FUNCTION

In quantum information theory, quantifying the dissimilarity between two quantum states is a fundamental problem. Various distance measures have been proposed, each with its unique properties and applications. One such measure is the trace distance, which captures the distinguishability between two quantum states [43]. Perez-Salinas et al. have analyzed the fidelity cost function with data re-uploading [1].

trace distance, particularly in the context of single-qubit systems, and discuss its potential as a cost function for quantum classifiers.

Despite the different mathematical formulations of trace distance and fidelity, these two measures share many similar properties and are widely used in the quantum computing and quantum information community. However, depending on the specific application, one measure may be more convenient or easier to work with than the other. This versatility and widespread adoption of both trace distance and fidelity in the field motivates our decision to discuss and compare these two important distance measures in the context of quantum classifiers. The trace distance between quantum states  $\rho$  and  $\sigma$  can be defined as,

$$D(\rho, \sigma) \equiv \frac{1}{2} \text{tr} |\rho - \sigma| \quad (2)$$

The trace distance between two single-qubit states, represented by their respective Bloch vectors  $\vec{r}$  and  $\vec{s}$ , is equal to one-half of the Euclidean distance between these vectors on the Bloch sphere. [43]

$$D(\rho, \sigma) = \frac{|\vec{r} - \vec{s}|}{2}. \quad (3)$$

This relation provides a geometric interpretation of the trace distance for single-qubit systems, linking it to the intuitive notion of distance in three-dimensional space.

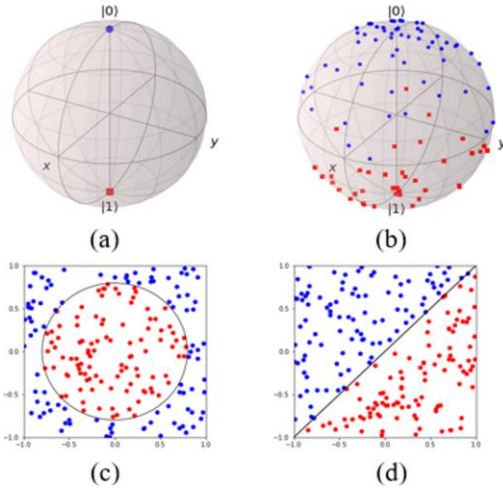


**FIGURE 3.** The single qubit classifier is trained to assign data points to one of two maximally orthogonal states on the Bloch sphere (a), denoted as  $|0\rangle$  and  $|1\rangle$ , which represent two distinct classes. Subplot (a) illustrates these target states for binary classification. Subplot (b) shows the classified data points mapped onto the Bloch sphere. Subplot (c) demonstrates a non-linear classification pattern, represented by a circle, with color-coded data points indicating their class assignments. Similarly, subplot (d) depicts a linear classification pattern, represented by a line, with color-coded data points denoting their respective classes.

However, the authors do not consider the case of the trace distance cost function, which is what we focus on in this section. We will explore the definition and properties of the

## III. UNIVERSALITY OF THE SINGLE-QUBIT CLASSIFIER

A key challenge in Quantum Machine Learning (QML) involves creating quantum circuits that efficiently handle complex tasks like classification without excessive use of quantum resources. The Universal Approximation Theorem (UAT) [44] is crucial for tackling this issue, demonstrating that a single-layer neural network with an appropriate activation function can approximate any continuous function to a desired accuracy, assuming enough hidden neurons are available. This UAT finds a compelling parallel in the quantum computing domain, particularly when considering the dynamics of quantum circuits. Here, the classical activation function is analogously performed by a unitary rotation acting upon a qubit. Specifically, a single-qubit quantum classifier, enhanced by the technique of data re-uploading, emerges as a universal approximator for any conceivable classification function. This universality hinges on the frequency of data re-uploading throughout the circuit's span [1], underscoring that even a solitary qubit is capable of encoding and processing multifaceted high-dimensional data. This is achieved through the execution of multiple rotations, each characterized by distinct angles and weights. The culmination of these processes is a final quantum state, which is then analyzed against a predefined target state correlating to each class. Optimization of the circuit's parameters is

pursued through the minimization of a cost function, which is indicative of the fidelity or trace distance between the comparative states.

By establishing the UAT within the context of quantum classifiers, a robust theoretical foundation is laid, alongside practical guidelines for the design and implementation of quantum circuits adept at sophisticated and non-linear classification tasks with minimal quantum resource expenditure. This breakthrough not only forges a theoretical link between quantum circuits and neural networks but also paves the way for innovative approaches in QML. Through this lens, quantum circuits are envisioned not merely as computational tools but as entities with the potential to parallel, and possibly surpass, the capabilities of their classical neural network counterparts, inspiring a new wave of methodologies in the realm of QML.

#### IV. OPTIMIZATION METHODS

In practice, deploying a parameterized quantum classifier involves a process of minimizing within the parameter space that delineates the circuit's configuration. The process is often termed a hybrid algorithm, denoting the symbiotic relationship and advantages derived from combining quantum logic and classical logic. In particular, the ensemble of angles ( $\theta_i$ ) and weights ( $w_i$ ) define a parameter space that requires systematic exploration to achieve the minimization of  $\chi^2$ .

The occurrence of local minima is unavoidable [2]. The arrangement of rotation gates results in a intricate multiplication of independent trigonometric functions, suggesting that our problem is characterized by a widespread distribution of minima.

The primary challenge boils down to minimizing a function that is defined by a vast array of parameters. In the case of a single-qubit classifier, the total number of parameters can be expressed as  $(3 + d)N$ , where  $d$  represents the problem's dimension (that is, the dimension of  $\mathcal{H}$ ), and  $N$  signifies the number of layers. Among these parameters, three are rotational angles, while the rest pertain to the weight [1]. To identify the most effective solution, we evaluate the performance of four distinct minimization techniques: the L-BFGS-B method, the COBYLA method, the Nelder-Mead method, and the Sequential Least Squares Programming (SLSQP) method.

The key challenge in optimizing a single-qubit classifier involves minimizing a function across a complex parameter space, calculated as  $(3 + d)N$ , where "d" is the problem's dimension and "N" the number of layers. Also in addition, we need to consider rotational angles and the weight ( $\bar{w}_i$ ) correspond to the dimension [1]. To discover the optimal solution, we delve into the efficiency of four diverse minimization strategies: the L-BFGS-B, COBYLA, Nelder-Mead, and Sequential Least Squares Programming (SLSQP) methods.

##### A. L-BFGS-B METHOD

The L-BFGS-B technique, part of the quasi-Newton optimization methods, refines the Broyden–Fletcher–Goldfarb–Shanno (BFGS) approach by efficiently using limited computer memory [45]. Its design excels in handling optimization tasks involving numerous variables, offering a linear memory usage advantage, making it highly effective for large-scale problems [46].

The L-BFGS-B method is widely recognized as a cornerstone technique across various advanced applications in the field of graphics [47, 48]. It specializes in minimizing a scalar function of one or several variables by initiating with a preliminary estimate of the optimum value. Through iterative refinement, it progressively improves upon this initial estimate to approach an optimal solution. The method employs function derivatives to determine the steepest descent's direction and to approximate the function's Hessian matrix (its second derivative), showcasing exceptional efficiency in matrix-vector multiplication operations [49].

##### B. CONSTRAINED OPTIMIZATION BY LINEAR APPROXIMATION METHOD

COBYLA (Constrained Optimization BY Linear Approximation) is an optimization algorithm designed to minimize a scalar objective function that depends on one or more variables, subject to constraints [50, 51]. One of the key features of COBYLA is that it does not require the calculation of derivatives, such as gradients or Hessians, of the objective function or constraints. This makes COBYLA particularly useful in situations where the derivatives are unknown, unreliable, or computationally expensive to obtain [50]. By relying on linear approximations of the objective function and constraints, COBYLA can effectively navigate the optimization landscape and find solutions even in the absence of explicit derivative information.

COBYLA has been effectively utilized in quantum computing, especially as a classical optimization routine within Variational Hybrid Quantum-Classical Algorithms (VHQCA) [52]. These algorithms employ a parameterized quantum circuit, or ansatz, which is refined through a dynamic interchange between a classical computer and a quantum device. The classical computer adjusts the ansatz's parameters to minimize a cost function, which the quantum device efficiently evaluates. Through iterative updates based on the cost function outcomes, the VHQCA aims to discover the most effective ansatz configuration for specific problems. The derivative-free characteristic of COBYLA makes it particularly advantageous for this setting, where the cost functions often lack easily computable or analytically defined derivatives.

##### C. NELDER-MEAD METHOD

The Nelder-Mead algorithm, introduced by John Nelder and Roger Mead in 1965, is a widely used direct search method

for unconstrained optimization problems [53]. The algorithm operates by maintaining a simplex of  $n+1$  points in an  $n$ -dimensional space, iteratively moving the simplex towards the optimal solution through a series of transformations, including reflection, expansion, contraction, and shrinkage [53].

Recent studies have focused on enhancing the Nelder-Mead algorithm to improve its efficiency and adaptability. Gao and Han [54] proposed an implementation of the Nelder-Mead algorithm with adaptive parameters, which can automatically adjust the parameter values based on the optimization progress. This adaptive approach has been shown to improve the algorithm's convergence speed and solution quality [54].

Its capacity to address problems in which derivative information is not readily accessible renders it a favorable option for numerous applications in QML. However, it is essential to conduct comprehensive evaluations to scrutinize the method's accuracy, efficiency, and sensitivity to the initial guess for each unique application [35, 55].

#### D. SEQUENTIAL LEAST SQUARES PROGRAMMING METHOD

The Sequential Least Squares Programming (SLSQP) method is an optimization technique that minimizes functions while adhering to specific constraints [56]. It is based on Sequential Quadratic Programming (SQP), which simplifies the optimization problem into a series of smaller, more manageable quadratic subproblems. In each subproblem, a quadratic approximation of the objective function and constraints is constructed using a second-order parabolic curve to model the function's behavior near a specific point. SLSQP updates this approximation using a quasi-Newton method.

Additionally, SLSQP applies a least-squares method to solve these quadratic subproblems, striving to minimize the total squared deviations between the approximation and actual function values. This method can handle both equality and inequality constraints, including variable bounds, by integrating a penalty function that imposes additional costs for any constraint or bound violations. SLSQP ensures efficient convergence by terminating the optimization process upon meeting a predefined convergence criterion, typically related to changes in the objective function value or the gradient vector's norm. This safeguard prevents indefinite computations, ensuring timely solutions.

Local minima are common challenges in both neural networks and quantum classifiers due to their complex mathematical structures—neural networks with compounded nonlinear functions and quantum circuits with prevalent trigonometric functions. This complexity increases the likelihood of encountering local minima during optimization. Moreover, with smaller training sets, the choice of optimization method is crucial. For instance, the Nelder-

Mead method is noted for its robustness, particularly its lower susceptibility to local minima.

It is also critical to recognize that minimization methods are sensitive to noise, which can significantly impact their effectiveness, especially in practical quantum computing applications [52].

## V. RESULT

In the field of QML, no comparative analysis has been conducted to evaluate the performance of four minimization methods- L-BFGS-B, COBYLA, Nelder-Mead, and SLSQP- on both fix and random datasets. Recognizing these gaps in the current research landscape, we introduce a novel approach that incorporates the trace distance cost function alongside the well-established fidelity cost function. Our study also extends its scope to include linear classification patterns, providing a more comprehensive understanding of the capabilities and limitations of quantum classifiers.

In this paper, we introduced two main cost functions (Fidelity and Trace distance), with two classification patterns (line and circle), as well as four minimization methods (L-BFGS-B, COBYLA, Nelder-Mead, and SLSQP). We concentrate on straightforward binary classification problems, such as distinguishing between circular and linear patterns. These tasks serve as benchmarks to thoroughly assess the performance of our classifiers and gain a meaningful understanding of their efficacy.

In our study, we meticulously construct a diverse array of algorithms by integrating various cost functions, classifiers, patterns, and minimization methods, aiming for a comprehensive evaluation of their capabilities, as shown in figure 4. To fine-tune these algorithms, we employ two distinct datasets: one consisting of fix data points and another comprising entirely random data points. This approach allows us to adjust the free parameters  $\theta_i$  and  $w_i$  across each layer effectively. Recognizing the limitations of fix datasets in mirroring complex real-world phenomena, we introduce a completely random dataset to challenge our classifier's adaptability and robustness. To account for the inherent variability of random data, we conduct each simulation 20 times, deriving an average accuracy rate to ensure statistical significance and reliability.

Central to our analysis is the application of these algorithms within the framework of a single qubit classifier, laying the groundwork for our comprehensive examination of each algorithm's performance. We specifically focus on benchmarking a selection of classifiers across varying numbers of layers, with a particular emphasis on configurations comprising five layers. This choice is predicated on the hypothesis that such an arrangement may unlock superior levels of performance and accuracy.

The subsequent sections delve deeper into this exploration, providing detailed insights into the performances of specific algorithms when implemented using single-qubit classifiers

with the innovative technique of data re-uploading. This methodical approach not only enhances our understanding of the single-qubit classifier's potential but also sets the stage for future advancements in the field of QML, spotlighting the critical role of algorithmic diversity and adaptability in navigating the complexities of quantum data classification.

#### A. EVALUATING NON-LINEAR AND LINEAR CLASSIFICATION APPROACHES FOR FIDELITY IN FIX AND RANDOM DATASETS

We generate a random dataset for circle classification pattern on a plane with coordinates  $\vec{x} = (x_1, x_2)$  with  $x_i \in [-1, 1]$  defined by a specific equation  $x_1^2 + x_2^2 < r^2$ , aiming to classify these points based on whether they fall inside or outside a circle of radius  $r = \sqrt{2/\pi}$ . The radius is chosen in a way that ensures equal areas for the regions inside and outside the circle. This setup results in a balanced dataset, where randomly assigning labels to data points would yield a 50 percent accuracy rate by chance.

In our study, we devised a methodology to assess the performance of a single-qubit classifier across various conditions by constructing a training dataset ranging from 1 to 50 randomly selected entries. The classifier's efficacy was then evaluated using a comprehensive test dataset consisting of 4000 points. To ensure uniformity across our experiments, a consistent seed was utilized for generating all data points in scenarios with fix data. Conversely, for analyses involving random data, data points were generated entirely at random for each of the 20 iterations to ascertain the average accuracy. We employed four different minimization methods to determine their effectiveness in maximizing accuracy for the same dataset, evaluated against two cost functions. This approach allowed us to identify the method that yields the highest accuracy with an equivalent number of training samples.

To facilitate our analysis, we generated a random dataset for a line classification problem, where the objective was to classify points on a plane, defined by  $\vec{x} = (x_1, x_2)$  with  $x_i \in [-1, 1]$  based on their position relative to a line defined by the equation  $y=x$ . The design of the line's function ensured that the probability of a data point being classified above or below it was equally likely, thus establishing a baseline success rate of 50% for random data point classification. To assess the performance of the single-qubit classifier, a training dataset containing a varying number of random samples, ranging from 1 to 50, is generated. The classifier's effectiveness is then evaluated using a fixed test dataset and a random test dataset, each comprising 4000 data points.

Before delving into the accuracy metrics of the 32 unique scenarios depicted in figure 4, we embarked on a preliminary analysis to identify an appropriate number of training

samples and layers. This preparatory step was crucial not only for establishing a consistent baseline for comparing training and test accuracies across various configurations but also for ensuring that our simulations remained feasible on our desktop computer with limited configurations. As illustrated in figures A1 and A2 in the Appendix, we conducted a series of runs with our algorithm, varying the number of layers from 1 to 5 and using up to 250 training

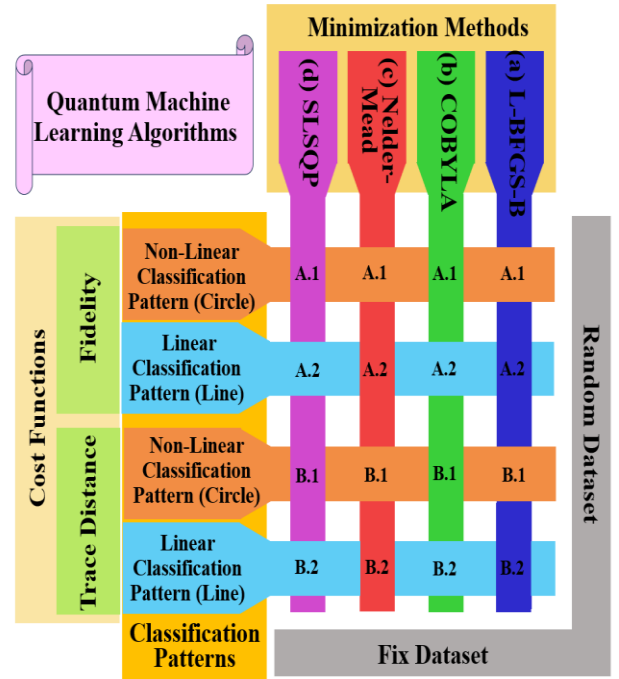


**FIGURE 4.** Schematics of 32 different cases are studied in this paper. It includes two cost functions, two classification patterns, and four minimization methods under two fix and random datasets. The detailed analysis and findings related to these methodologies are systematically organized in the manuscript under sections A.1, A.2, B.1, and B.2, providing a structured overview of our approach and results.

samples, to determine the conditions under which our algorithm would reach a test accuracy around 90%. This exploration led us to conclude that training samples ranging from 60 to 250 and 5 layers were suited for our studies. To maintain a uniform evaluation framework, we subsequently used these values for all simulated cases.

#### 1) NON-LINEAR CLASSIFICATION PATTERN (NLCP) FIDELITY FOR FIX AND RANDOM DATASETS:

Figure 5 illustrates a comparison of four distinct optimization techniques, namely L-BFGS-B, COBYLA, Nelder-Mead, and SLSQP, applied to the task of classifying the circle pattern. The comparison evaluates both training and test accuracies using a fix dataset of 4000 test samples and 5 layers.

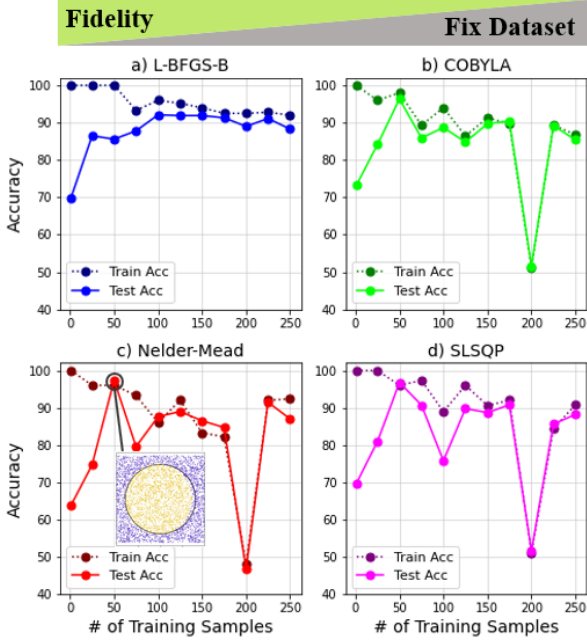


**FIGURE 5.** Train and test accuracy of fidelity for the 5-layer model of circle classification and fix dataset for (a) L-BFGS-B, (b) COBYLA, (c) Nelder-Mead and (d) SLSQP minimization methods to represent A.1 category in figure 4. The inset image in subplot (c) in the graph shows a visualization of a circle classification task with the highest accuracy of 95% in the Nelder-Mead minimization method.

Initially, all algorithms demonstrate a perfect training accuracy of 100% with just a single sample, a result that aligns with expectations. However, as we increase the sample size, a divergence in performance becomes evident for these four minimization methods. The L-BFGS-B method maintains a training accuracy close to 90%, showcasing its robustness against overfitting. In contrast, COBYLA, Nelder-Mead, and SLSQP show significant variability and a decline in training accuracy, indicating a susceptibility to overfitting. Specifically, the test accuracy for these three methods displays considerable fluctuations, with the Nelder-Mead method experiencing a pronounced dip below 50% accuracy when utilizing 200 training samples. This point marks a notable decrease in performance for COBYLA, Nelder-Mead, and SLSQP, possibly hinting at optimization challenges such as becoming trapped in local minima when handling larger datasets. Interestingly, the peak accuracy for COBYLA, Nelder-Mead, and SLSQP is achieved with merely 50 samples, beyond which overfitting becomes a significant issue. This observation suggests that, unlike L-BFGS-B, which requires a minimum of 100 samples to achieve the accuracy of 92%, the other three methods can attain over 95% accuracy with only 50 samples. L-BFGS-B does not reach this high accuracy level at 100 samples, and its performance slightly declines with an increase in training samples after 150 training samples. This analysis highlights

the critical importance of carefully selecting the number of training samples based on the minimization method used. The right choice can effectively prevent overfitting, thereby enhancing classification accuracy. This insight is crucial for optimizing machine learning models and ensuring their generalizability and efficiency in practical applications.

Figure 6 delves into the accuracy of these four distinct minimization methods —L-BFGS-B, COBYLA, Nelder-Mead, and SLSQP— when applied to a fidelity cost function and a random dataset for circle classification. This analysis underscores a consistent trend across all methods: an initial increase in test accuracy corresponding to the rise in the number of training samples, yet fails to surpass a peak accuracy of 90%. This trend highlights the inherent challenges faced by these minimization methods when dealing with random datasets. In the L-BFGS-B method as depicted in figure 6(a), showcases a notable performance, achieving its highest test accuracy of 88.8% with 35 training samples. This point also marks the narrowest gap of 5% between training and test accuracy, indicating a relatively high level of model efficiency and generalization at this sample size. However, as the analysis progresses, it becomes apparent that increasing the number of training samples beyond this optimal point does not translate to improved performance. The gap between the train and test accuracy remains notably constant at around 10% even as the sample size is increased to 70 training samples. Transitioning to the COBYLA method, as depicted in figure 6(b), a different performance pattern emerges. Contrary to L-BFGS-B, COBYLA achieves its best test accuracy at 84.8% with a higher training sample equal to 70. This method experiences fluctuations, yet it is noteworthy that the gap between training and test accuracies exhibits a decreasing trend, suggesting a gradual improvement in model generalization compared to the initial stability seen with L-BFGS-B. Figure 6(c) focuses on the Nelder-Mead method, highlighting a decrease in the gap between training and test accuracies as the number of training samples increases, culminating in a maximum accuracy of 86.9% with 60 training samples. Figure 6(d) examines the SLSQP method, which shows an increase in test accuracy up to 50 training samples before demonstrating a decline in both training and test accuracies. This shows the SLSQP method is more prone to overfitting. The SLSQP method reaches a maximum accuracy of 86.7% when applied to a dataset of 50 samples. These results, as detailed in Figure 6, provide vital insights into the performance of various minimization methods when working with a fidelity cost function and a random dataset. The diverse outcomes emphasize the importance of choosing an optimal number of training samples to prevent overfitting and enhance accuracy. This underlines the delicate balance needed to fully leverage these computational methods in practical scenarios.

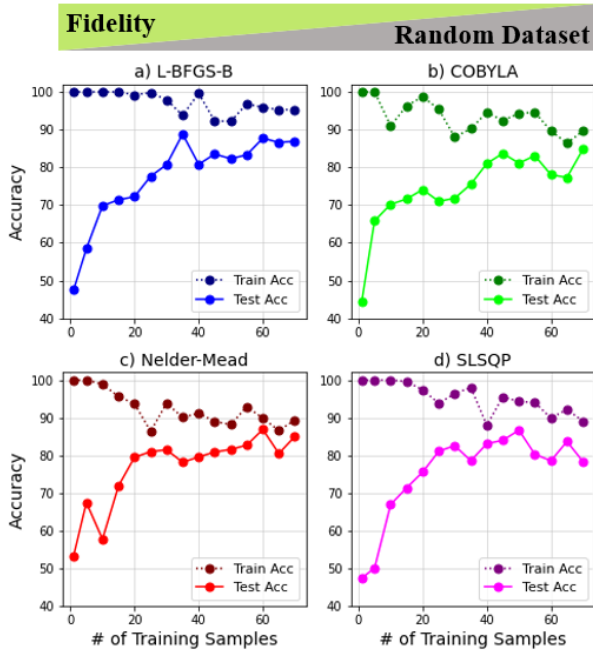


**FIGURE 6.** Train and test accuracy of fidelity for the 5-layer model of circle classification and random dataset for (a) L-BFGS-B, (b) COBYLA, (c) Nelder-Mead and (d) SLSQP minimization methods to represent A.1 category in figure 4.

## 2) LINEAR CLASSIFICATION PATTERN (LCP) FIDELITY FOR FIX AND RANDOM DATASETS:

Figure 7 illustrates a comparison of four different optimization techniques applied to the task of classifying line patterns, using fidelity-based cost function and the fixed dataset. The subplot (a) focuses on the performance of the L-BFGS-B method. Here, the training accuracy starts at a perfect 100% and impressively remains above 97% even as the number of training samples increases. Conversely, the test accuracy initiates at a relatively lower rate of 62.2% with just a single sample yet it progressively improves, reaching approximately 95% accuracy with 75 training samples and slightly declines for larger training samples. An initial notable gap between the training and test accuracy is evident, but this gap diminishes significantly as the dataset expands with more training data, indicating an improvement in the model's ability to generalize from the training to the unseen test data. The subplot (b) depicts the results obtained using the COBYLA algorithm, which exhibits a performance pattern similar to that of the L-BFGS-B method, consistently achieving 100% accuracy on the training data. The accuracy on the test set starts at 66.9% and steadily improves as more training samples are added, ultimately reaching 95% when 125 samples are used for training. The disparity between training and test set accuracies mirrors the pattern observed with the L-BFGS-B method, consistently manifesting across all training dataset sizes. The Nelder-Mead approach, shown in figure 7(c), achieves a notable test accuracy of 97.7% with 125 training samples. The inset provides a graphical

visualization of line classification using this minimization method at this specific point, illustrating that the line classification performance is exceptionally well. The visualization clearly demonstrates the method's effectiveness in accurately separating the data points into distinct classes, highlighting the Nelder-Mead method's precision and robustness in handling line classification tasks with a substantial number of training samples. Furthermore, the training and test accuracy curves show a notably smaller gap, converging to the same value with training sets of 100 and 125 samples. The final subplot (d) evaluates the performance of the SLSQP method, which closely aligns with the results from the COBYLA method. The test set accuracy exhibits a progressive increase, rising from 62.7% to 96.6%. The disparity between the training and test accuracies is similar to that observed with the COBYLA method. In summary, all four optimization techniques demonstrate a reduction in overfitting as the training dataset size increases, ultimately achieving a test accuracy of at least 95% when training with 125 samples for this line classification task.

Figure 8 showcases an analysis of the classification accuracy obtained using the same minimization methods across random datasets. Consistently, a rise in the number of training samples correlates with an increase in test accuracy across all methods evaluated. Notably, with just 50 training samples, all methods surpass the 90% accuracy threshold. Specifically, in figure 8(a), the L-BFGS-B method reaches the peak accuracy of 92.8% with 50 training samples. It was observed that as the number of samples increased, the disparity between train and test accuracies for the L-BFGS-B method began to narrow, although this gap persisted in being slightly wider than that observed in the other methods. Figure 8(b) demonstrates that the COBYLA method, with the same number of samples, attains a superior accuracy of 93.5%. This suggests that COBYLA not only reaches high classification accuracy with a minimal dataset but also demonstrates better generalization compared to L-BFGS-B, as reflected by the narrower gap between its training and test accuracies. Figure 8(c) examines the Nelder-Mead method, showing its peak accuracy of 93% with 40 training samples, after which its accuracy slightly declines. Interestingly, the smallest disparity between training and test accuracies—only 1.8%—occurs in 50 training samples. Despite slightly lower accuracy at this point, this smallest gap signifies that the Nelder-Mead method achieves a remarkable balance between learning from the training data and generalizing to unseen data, highlighting its efficiency and potential for precise model tuning. Figure 8(d) illustrates that the SLSQP method achieves an impressive peak test accuracy of 96.4% for line classification using a random dataset, attained with 45 training samples. At this juncture, the discrepancy between training and test accuracies is notably small, indicating a high level of model precision and generalization. Like the Nelder-Mead method, the SLSQP method exhibits a nonmonotonic increment in test accuracy as a function of training samples,

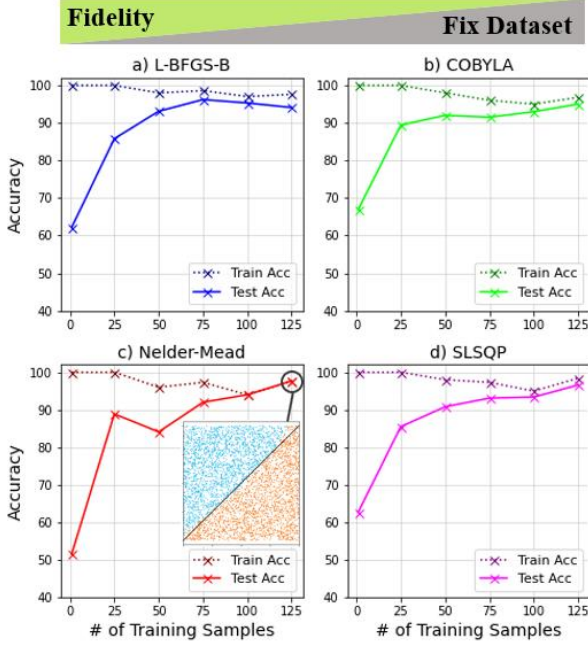


**FIGURE 7.** Train and test accuracy of fidelity for the 5-layer model of line classification and fix dataset for (a) L-BFGS-B, (b) COBYLA, (c) Nelder-Mead and (d) SLSQP minimization methods to represent A.2 category in figure 4. The inset graph in subplot (c) shows the visualization of a line classification pattern with the highest accuracy of 97.7% in the Nelder-Mead minimization method.

as indicated by the irregular slope of test accuracy. This fluctuation suggests that for these methods, adding more training samples does not straightforwardly translate to higher test accuracies, highlighting the complexity of optimizing model performance across different minimization techniques.

A comparison of Figures 5 and 7 reveals that the accuracy curves for line classification are more stable and consistent across all optimization techniques when compared to those for circle classification. The accuracy values for classifying circle patterns display greater variability and fluctuations than those observed in the line classification task. The observed differences in performance between circle and line classification could stem from several technical factors: (1) Line classification likely represents a more straightforward pattern that aligns better with the linear decision boundaries most classifiers are adept at identifying. In contrast, circle classification involves recognizing more complex, non-linear patterns, which can challenge the classifiers' ability to generalize from the training data without overfitting or underfitting. (2) The algorithms applied for circle classification might be more prone to getting trapped in local minima due to the more intricate decision boundaries required to accurately classify circular patterns. This can hinder the optimization process, leading to increased fluctuations in classification accuracy as the model struggles to find the global optimum. (3) The differences in performance may also reflect the inherent adaptability of the

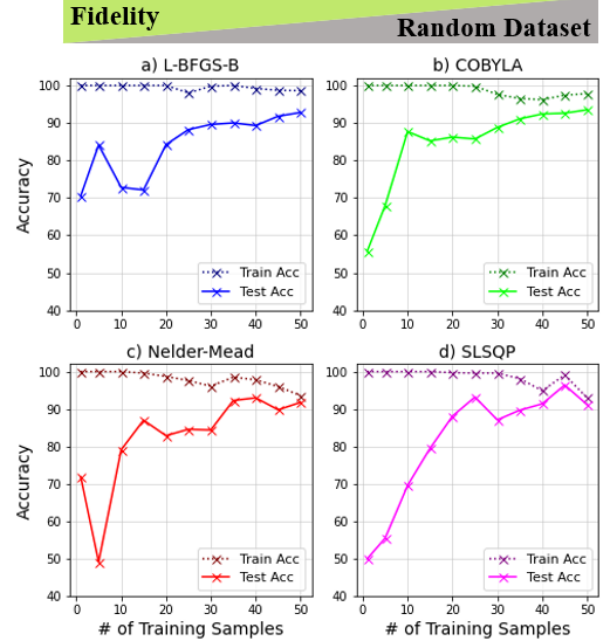


**FIGURE 8.** Train and test accuracy of fidelity for the 5-layer model of line classification and random dataset for (a) L-BFGS-B, (b) COBYLA, (c) Nelder-Mead and (d) SLSQP minimization methods to represent A.2 category in figure 4.

algorithms to the specific types of classification tasks with the geometric properties. A comparative analysis of Figures 6 and 8 indicates that the specific characteristics of the classification problem significantly affect the potential to attain higher accuracy with fewer samples. The fluctuations in the line classification pattern are less pronounced than those in the circle classification pattern. This observation underscores the importance of selecting appropriate optimization methods based on the complexity of the classification problem.

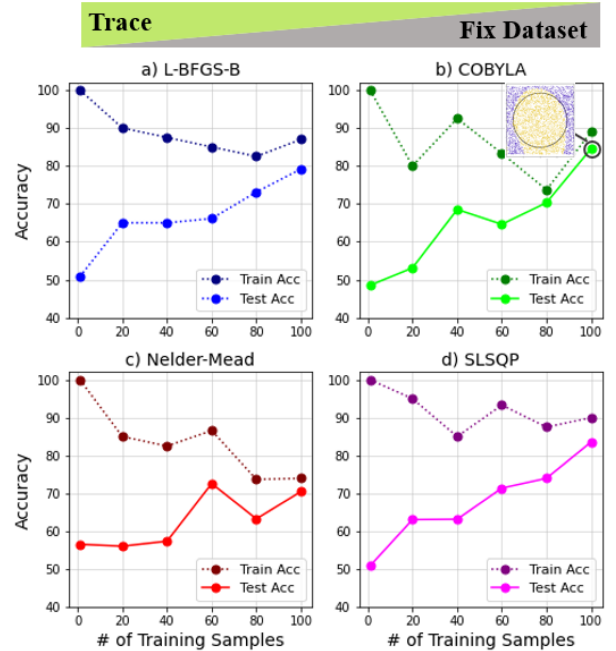
## B. EVALUATING NON-LINEAR AND LINEAR CLASSIFICATION APPROACHES FOR TRACE DISTANCE IN FIX AND RANDOM DATASETS

### 1) NLCP TRACE DISTANCE FOR FIX AND RANDOM DATASETS:

Figure 9 showcases the effectiveness of the trace distance cost function in classifying circular patterns within a fix dataset. In subplot (a), the L-BFGS-B minimization method achieves its highest test accuracy at 79.2% with a dataset comprising 100 training samples. Subplot (b) examines the performance of the COBYLA method, which displays greater variability in training accuracy than L-BFGS-B but ultimately achieves a higher peak test accuracy of 84.6%, also with 100 training samples. Notably, COBYLA demonstrates enhanced generalization capabilities relative to other methods, as indicated by the narrower margin between its training and testing accuracies. This performance suggests that, when applied alongside the trace distance cost function, the COBYLA method is particularly adept at optimizing

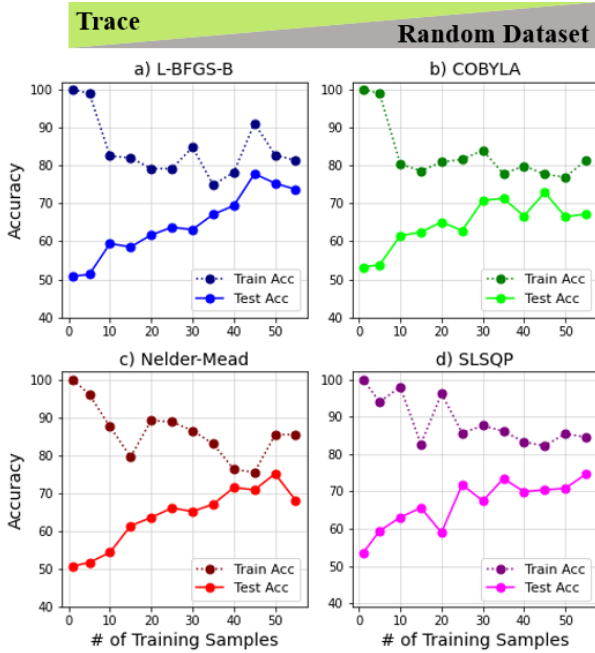
parameters for improved generalization to unseen testing data. An accompanying visualization within the inset illustrates the classification of circular patterns at this accuracy peak. In subplot (c), the analysis shifts to the performance of the Nelder-Mead method, which records its optimal test accuracy at 72.6% utilizing 60 training samples. This method exhibits signs of overfitting, a condition where the model learns the training data too closely and fails to generalize well to new, unseen data. Despite a narrowing gap between training and testing accuracies as the number of training samples grows, a concurrent decline in training accuracy is observed, which adversely affects the overall test accuracy. This pattern suggests a limitation in the Nelder-Mead method's capacity to effectively handle the trace distance cost function, likely due to its inherent characteristics such as reliance on simplex-based optimization, which might struggle with the complexity of the trace distance landscape. Consequently, this method appears less suited for tasks requiring robust generalization from the trace distance cost function, particularly in scenarios demanding accurate classification of complex patterns with a limited dataset. In subplot (d), the focus turns to the SLSQP method which attains its peak test accuracy at 83.6% with a dataset of 100 training samples. The disparity between training and testing accuracy contracts by increasing the training samples, indicating an improvement in the model's ability to generalize from the training to the testing dataset. However, even at the point of 100 training samples, the gap between training and testing accuracies, while reduced, remains significant. This persistent gap suggests that while the SLSQP method is effective at learning and generalizing from the given data, there is still a margin for optimization to further bridge the difference in accuracies. Each optimization technique successfully minimizes the cost function and attains perfect accuracy on the training set using a comparatively small number of samples. However, their performance varies considerably when it comes to generalizing to the test set. This highlights the crucial role played by the choice of optimization algorithm in determining the overall effectiveness of the model. In conclusion, when considering the fixed dataset and the trace distance cost function, the COBYLA method demonstrates superior performance in optimizing the parameters to generalize effectively to unseen test data. Compared to the other techniques evaluated, it necessitates fewer training samples to achieve satisfactory accuracy on the test set.

Figure 10 illustrates how the accuracy on both the training and test sets evolves as the number of training samples grows, specifically for the task of classifying circular patterns using the trace distance cost function, evaluated on a randomly generated dataset. Similar to all scenarios analyzed so far, a common pattern emerges where test accuracy begins at a relatively low level for all minimization methods but demonstrates a consistent increase as more training data is provided. This trend highlights the methods' capacity to



**FIGURE 9.** Train and test accuracy of trace distance for the 5-layer model of circle classification and fix dataset for (a) L-BFGS-B, (b) COBYLA, (c) Nelder-Mead and (d) SLSQP minimization methods to represent B.1 category in figure 4. The inset graph in subplot (b) shows the visualization of a circle classification pattern with the highest accuracy of 84.6% in the COBYLA minimization method.

effectively learn distinguishing features, thereby enhancing their ability to generalize to unseen data. Specifically, in subplot (a), the L-BFGS-B method illustrates impressive learning efficiency, with test accuracy exceeding 70% after incorporating just 40 training samples and achieving its highest test accuracy of 77.8% with 45 training samples. In subplot (b), the COBYLA method's performance is slightly lower compared to L-BFGS-B, plateauing at a test accuracy of 72.8% with 45 training samples. This performance indicates that while COBYLA may be susceptible to some degree of overfitting, it nonetheless achieves a reasonable level of generalization. Subplot (c) explores the Nelder-Mead method, which reaches its peak test accuracy of 75.1% with 50 training samples. Subplot (d) utilizes the SLSQP method, which shows fluctuations in its training accuracy remaining above 80%. The test accuracy for SLSQP was enhanced significantly, reaching 74.6% with 50 samples. This fluctuation and eventual rise in test accuracy underscores the method's potential for optimizing classification tasks, despite the initial variability. In sum, the L-BFGS-B method stands out for achieving the highest test accuracy among the methods evaluated, requiring only 45 training samples to reach this optimum on a random dataset. Summarily, employing the trace distance cost function across these various minimization strategies yields test accuracy ranging from 65% to 78% on the random dataset, illustrating the function's effectiveness and the distinct performance capabilities of each minimization method.



**FIGURE 10.** Train and test accuracy of trace distance for the 5-layer model of circle classification and random dataset for (a) L-BFGS-B, (b) COBYLA, (c) Nelder-Mead and (d) SLSQP minimization methods to represent B.1 category in figure 4.

## 2) LCP TRACE DISTANCE FOR FIX AND RANDOM DATASETS:

Figure 11 offers a comparative analysis of the accuracy achieved by four different optimization methods when applied to a trace distance cost function for line pattern classification using a fixed dataset. Subplot (a) highlights the L-BFGS-B method, showcasing its high level of stability in training accuracy. The test accuracy shows a steady increase, reaching 91.8% with 100 training samples. While there is a substantial gap between the accuracies of the training and test sets at the outset, this difference gradually narrows as more training samples are introduced. This highlights the L-BFGS-B method's capacity to adapt and learn more complex patterns effectively, demonstrating robustness and in leveraging larger datasets for improved generalization. The subplot (b) illustrates the results obtained using the COBYLA method. In contrast to the L-BFGS-B approach, the accuracy on the training set shows greater fluctuations, even experiencing a drop to 56.9% at one instance before rebounding. The test accuracy follows a similar pattern to that seen in L-BFGS-B, beginning at 49.8% and increasing to 87.4%. Once the training set size reaches 80 samples, both the training and test accuracies seem to reach a plateau, slightly below the 90% mark. In subplot (c), the Nelder-Mead method starts with a modest test accuracy of 55.3%, which significantly improves to 87% with the addition of 60 training samples demonstrating a similar trend as the L-BFGS-B method. Initially, a pronounced gap exists between training and test accuracies, which persists until the dataset is expanded to include 80 training samples. Beyond this point,

the sign of overfitting emerges, as demonstrated by a decline in training accuracy while test accuracy plateaus. For 100 training samples, the test accuracy interestingly becomes 2% higher than the training accuracy, indicating a unique inversion where the model performs slightly better on unseen data than on the training set itself, a rare occurrence that may suggest the model has reached a point of optimization where it generalizes exceptionally well to new data. The subplot (d) of Figure 11 presents the results of the SLSQP method. Notably, this technique achieves the highest accuracy on the test set, reaching 93.3% using just 40 training examples. The SLSQP method appears to be the most appropriate choice for trace distance classification tasks, as it exhibits a smaller discrepancy between its performance on the training and test datasets. The inset provides a visual representation of the SLSQP's performance at this specific point. To summarize, all optimization methods demonstrate an upward trajectory in test accuracy as the size of the training dataset increases, suggesting enhanced generalization capabilities of the model. Among the four techniques evaluated, the SLSQP method seems to strike the most favorable balance between its performance on the training and test sets.

Figure 12 presents a comparison of different optimization techniques when applied to the task of classifying line pattern using a randomly generated dataset and a cost function based on trace distance. In subplot (a), we examine the performance of the L-BFGS-B method, which attains its peak test accuracy of 86.3% with 55 training samples. Before reaching this point, the method's test accuracy demonstrated considerable variability, oscillating between 70% and 80% as the number of training samples ranged from 20 to 50. However, a notable improvement occurs when the dataset is expanded to 55 training samples, at which the test accuracy leaps to 86.3%, effectively surpassing the earlier fluctuation band. This pivotal moment also marks the occurrence of the smallest gap between training and test accuracies, showcasing a significant enhancement in the model's ability to generalize from the training dataset to unseen data, thereby achieving an optimal balance at this specific training sample size. Subplot (b) delves into the efficacy of the COBYLA optimization method, which achieves its highest test accuracy of 86.8% with a relatively smaller dataset of 35 training samples. Beyond this optimal threshold, signs of overfitting become apparent, as both training and test accuracies start to decline. This pattern suggests that while the COBYLA method is highly effective up to a certain point, adding more training samples beyond this number paradoxically hampers the model's performance. The decline in accuracy indicates that the model begins to memorize the training data rather than learning to generalize, leading to a decrease in its ability to accurately predict outcomes on unseen data. This observation underscores the importance of identifying the ideal number of training samples to maximize the effectiveness of the COBYLA method without crossing into the territory of

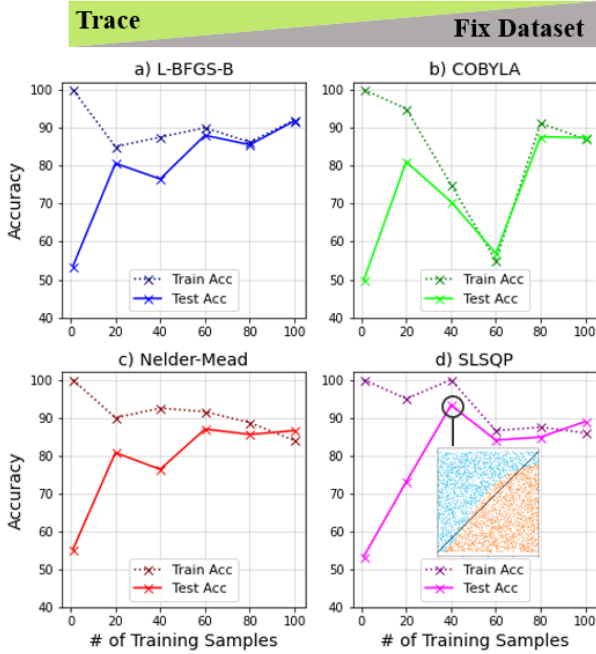


**FIGURE 11.** Train and test accuracy of trace distance for the 5-layer model of line classification and fix dataset for (a) L-BFGS-B, (b) COBYLA, (c) Nelder-Mead and (d) SLSQP minimization methods to represent B.2 category in figure 4. The inset graph in subplot (c) shows the visualization of a line classification pattern with the highest accuracy of 93.3% in the SLSQP minimization method.

overfitting. In subplot (c), the focus is on the Nelder-Mead optimization method, which shows some fluctuations in performance before reaching its maximum test accuracy. It successfully achieves a test accuracy of 88.1% with 40 training samples. However, akin to the pattern observed with the COBYLA method, the Nelder-Mead method also sees a decline in both training and test accuracies when additional training samples are added beyond this optimal number. This decline serves as a clear indication of the onset of overfitting, suggesting that while the Nelder-Mead method can efficiently utilize a certain number of training samples to improve its predictive accuracy, exceeding this number leads to a reduction in model performance. In subplot (d), a more continuous and stable increase in test accuracy is observed with each increase in the number of training samples. This trend results in the highest test accuracy being recorded at 88.3% with 55 training samples. Unlike the previous methods discussed, this subplot suggests a method that maintains its efficiency and ability to generalize well without showing immediate signs of overfitting up to this point. The gradual and consistent improvement in test accuracy highlights the method's effective learning curve and suggests an optimal balance between learning from the training data and applying this knowledge to unseen data.

Figure 13 offers a comparative analysis of the highest accuracies achieved for two distinct classification patterns – linear (line) and non-linear (circle) – across the four distinct minimization methods when applied to both random and fix

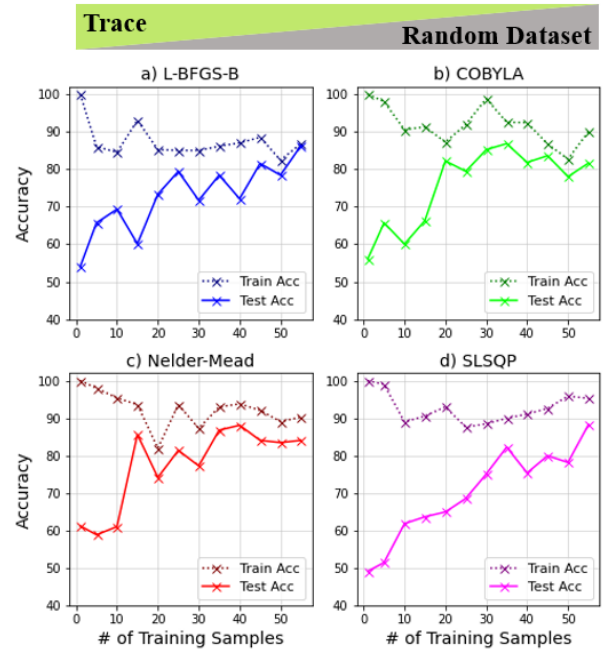


**FIGURE 12.** Train and test accuracy of trace distance for the 5-layer model of line classification and random dataset for (a) L-BFGS-B, (b) COBYLA, (c) Nelder-Mead and (d) SLSQP minimization methods to represent B.2 category in figure 4.

datasets within the context of a fidelity cost function. The analysis reveals a notable trend: in circle classification tasks, the fix dataset consistently yields higher accuracies than their random counterparts for all tested minimization methods. This suggests that the inherent geometric complexities of non-linear patterns may align more closely with the simpler structure of fix datasets, thereby facilitating more accurate classification. Similarly, for line classification, the fix dataset leads to enhanced accuracies with the L-BFGS-B and SLSQP methods, indicating these methods' effectiveness in leveraging structured data to accurately discern linear relationships. However, the random dataset achieves better accuracy when classified using the Nelder-Mead method. This could suggest that the Nelder-Mead method, known for its simplicity and direct search approach, might be particularly adept at navigating the stochastic nature of random datasets to identify linear patterns. Across all algorithms, the task of classifying non-linear patterns, especially within random datasets, emerges as inherently challenging. This complexity likely stems from the algorithms' varying abilities to parse and learn from the unpredictable variance found in random datasets, as well as the added difficulty of accurately modeling non-linear relationships. The findings underscore the critical importance of selecting the appropriate minimization method based on the dataset's nature and the classification task's geometric complexity to optimize classification accuracy.

Figure 14 provides the performance comparison of two distinct classification patterns—line and circle—across four different minimization methods when applied to both random

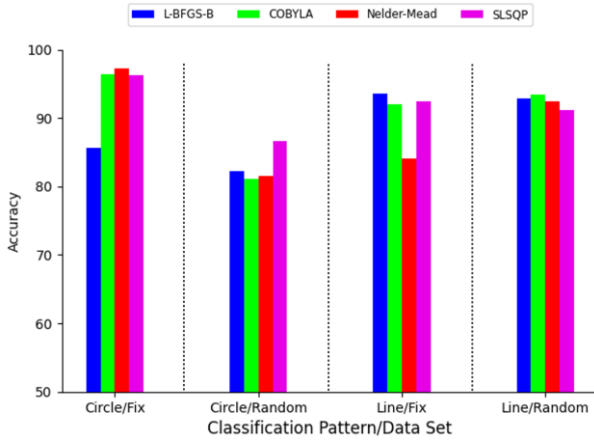


**FIGURE 13.** comparison the result of test accuracy of the 5-layer model of fidelity cost function for linear and non-linear classification patterns for random and fix datasets in four minimization methods across 50 samples.

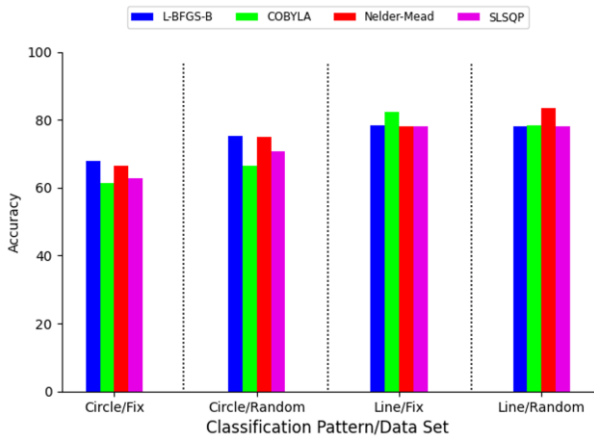


**FIGURE 14.** Evaluating of trace distance test accuracy of 5-layer model across 50 samples for linear and non-linear classification problems for random and fix datasets in four minimization methods.

and fix datasets, this time employing the trace distance cost function. A pivotal observation emerges when comparing the performance of circle classification with a fix dataset (circle/fix) against the fidelity cost function results presented in figure 13. It is evident that the accuracies achieved using the trace distance cost function are notably lower across all minimization methods compared to those obtained with the fidelity cost function. This discrepancy highlights the inherent challenges and differences in how each cost function interacts with the underlying data and the classification task at hand. The trace distance cost function, known for quantifying the distinguishability between quantum states, may present a more complex landscape for optimization, particularly when applied to classical data patterns such as lines and circles. This complexity could lead to lower classification accuracy as the minimization methods struggle to navigate the nuances of the trace distance landscape effectively. Such an observation underscores the importance

of cost function selection in machine learning tasks, emphasizing that the choice of cost function can significantly impact the model's ability to learn and generalize from the data. The comparative analysis in figure 14 serves as a testament to the nuanced interplay between cost functions, dataset types (fix vs. random), and the geometric nature of the classification patterns, offering valuable insights into optimizing classification accuracy through strategic method and cost function selection.

In addition, the fix dataset achieves superior accuracy specifically when employing the COBYLA minimization method, indicating a unique synergy between COBYLA's optimization strategy and the structured nature of fix datasets for linear patterns. Conversely, for the random dataset, there's a notable trend where it consistently outperforms the fix dataset across all other minimization methods, suggesting that the stochastic characteristics of random datasets may be better suited to the optimization landscapes these methods navigate, particularly for linear classifications. In circle classification tasks, the random dataset not only demonstrates improved accuracy over the fix dataset for all minimization methods but also reinforces the observation that random datasets generally offer a more favorable context for the trace distance cost function across both classification patterns. This enhancement in accuracy with random datasets could be attributed to the trace distance cost function's sensitivity to the variances within the dataset, allowing for more effective differentiation and classification of non-linear patterns like circles when the data is less predictable.

## VI. CONCLUSION

This work presents a pioneering investigation into enhancing quantum classifier performance through strategic data re-uploading, exploring its impact across both linear and non-linear classification paradigms. By integrating novel cost functions and employing various optimization methods, we significantly advanced the accuracy and robustness of quantum classifiers. Our approach, which leverages the unique properties of quantum mechanics, demonstrates substantial improvements over traditional models, particularly in handling complex patterns within minimal datasets. Through comprehensive comparisons across diverse datasets and classification tasks, we underscore the adaptability of our methodology to different learning scenarios, thereby offering a versatile tool for QML applications.

Our findings contribute to the theoretical foundations of QML and provide practical insights into the design and optimization of quantum classifiers. The exploration of different cost functions reveals their distinct impacts on model performance, highlighting the importance of careful selection based on the task at hand. Furthermore, our study illustrates the effectiveness of data re-uploading in enhancing model expressivity, a key factor in achieving high classification accuracy with fewer training samples.

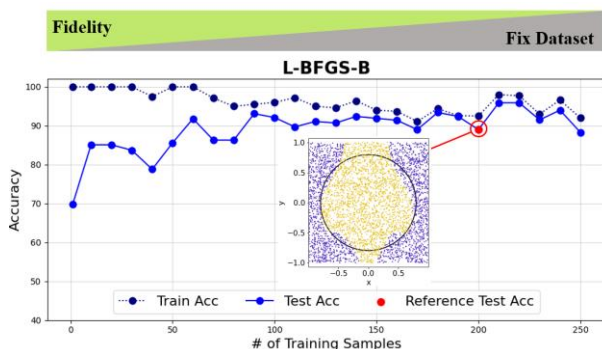
Future work will focus on extending these methodologies to more complex quantum systems and exploring their application in broader quantum computing tasks. By continuing to unravel the capabilities of quantum classifiers and refining their design, we move closer to realizing the full potential of quantum computing in addressing some of the most challenging problems in machine learning and beyond. During the paper, we mention some of the results from computational speed which shows promising, and we will consider it for our next papers.

This research not only paves the way for further advancements in QML but also highlights the transformative impact quantum computing can have across various scientific and technological domains.

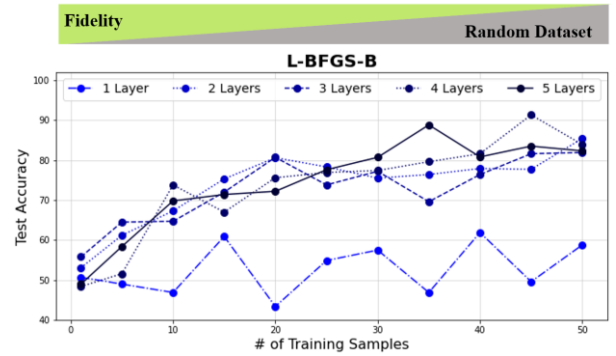
## APPENDIX

Figure A1 illustrates the performance of a quantum classifier utilizing a fidelity cost function within a five-layer framework for circular pattern classification in a fix dataset, employing the L-BFGS-B optimization method. The analysis encompasses training data up to 250 samples to benchmark our algorithm against the findings from reference [1]. The diagram depicts training accuracy with a blue dashed line and test accuracy with a solid blue line, underscoring the algorithm's efficacy. A red dot highlights a notable benchmark from the reference, showing an 89% accuracy with 200 training samples, demonstrating parity with this published result. The inset provides a visual representation of the classification process. Notably, test accuracy begins at approximately 70%, rising impressively to 96% for a slightly expanded dataset of 210 samples. Remarkably, with as few as 60 training samples, the model achieves a test accuracy of 91.8%, and the discrepancy between training and test accuracy diminishes with the inclusion of 90 samples. This observation underscores the efficiency of our approach, highlighting its capability to reach high accuracy levels without necessitating extensive training data.

Figure A2 showcases a systematic evaluation of a circular pattern classification model across a spectrum of architectural depths, ranging from 1 to 5 layers. The graphical analysis reveals that models with a solitary layer lag in performance compared to those with increased layer



**FIGURE A1.** Train and test accuracy of fidelity for the 5-layer model of circle classification and fix dataset for L-BFGS-B minimization method. The inset graph shows the visualization of a nonlinear classification reported on [1].



**FIGURE A2.** Evaluate the test accuracy of fidelity for circle classification and random dataset for L-BFGS-B minimization method, ranging from 1 to 5 layers.

counts, marking a clear trend: as the number of layers escalates, so does the model's classification accuracy. Specifically, a single-layer setup achieves a peak accuracy of 61.9%, whereas a more complex five-layer configuration significantly elevates this metric to 88.8%, even when limited to only 35 training samples. This observation underscores a critical insight—enhancing the model's depth systematically improves its predictive capabilities, a phenomenon consistent with the advantages afforded by the data reuploading strategy integral to our approach. Given this marked improvement in model efficacy with layer augmentation, the paper prioritizes an in-depth investigation and discourse on the five-layer model's architecture, focusing on its ability to optimize classification accuracy with efficient utilization of training data.



**Sara Aminpour** Sara Aminpour is currently pursuing her Ph.D. at the School of Electrical and Computer Engineering, in conjunction with the Center for Quantum Technology, at the University of Oklahoma. With a Master's degree in Physics, her thesis on the "Data Classifier Based on No-Cloning Theorem" has robustly paved the way for her burgeoning research interests in quantum technology. Sara is an active member of the IEEE society, contributing to the advancement of her field through rigorous research and scholarly discourse. Her dedication to the field of Physics and Engineering is evident in her academic achievements and ongoing research endeavors.



**Yaser Mike Banad**, (Chair of Computer Society in IEEE Oklahoma City Chapter), is an Associate Professor at the School of Electrical and Computer Engineering, University of Oklahoma, holds M.Sc. and Ph.D. degrees in electrical and computer engineering from

Louisiana State University (2016). An author of over 100 peer-reviewed publications, Dr. Banad's research spans neuromorphic computing, energy-efficient devices and circuits design, neural-inspired artificial intelligence acceleration, and material analysis for semiconductor technologies. He directs the Neuromorphic Intelligent Computing Systems (NICS) lab at OU, dedicated to advancing reliable, energy-efficient neuromorphic engineering from materials and devices to systems, algorithms, and applications.



**Sarah S. Sharif**, (Chair of Young Professional in IEEE OKC), is an assistant professor in the School of Electrical and Computer Engineering at the University of Oklahoma since 2022. In addition, she is a distinguished faculty member at the Center for Quantum Research and Technology at the same institution. Before joining OU, she was a postdoctoral research associate at the University of Illinois Urbana-Champaign. Her research during her Ph.D. focused on developing Stochastic Optimization and Machine Learning Techniques for Photonic Nanostructures and Quantum Optical Systems. She holds a Ph.D. in Electrical Engineering with a minor in Physics and two M.Sc. degrees in Natural Science (Physics) and Electrical Engineering. Additionally, she has a graduate certificate in Material Science. She leads the Quantum Nanophotonic Engineering Technology & System (QNETS) group at OU, focusing on the development of next-generation computing and sensing technologies through optical, quantum optical devices and system, including quantum machine learning, quantum information, and quantum communication.

- [1] A. Pérez-Salinas, A. Cervera-Lierta, E. Gil-Fuster, and J. I. Latorre, "Data re-uploading for a universal quantum classifier," *Quantum*, vol. 4, p. 226, 2020.
- [2] M. Cerezo, G. Verdon, H.-Y. Huang, L. Cincio, and P. J. Coles, "Challenges and opportunities in quantum machine learning," *Nature Computational Science*, vol. 2, no. 9, pp. 567-576, 2022.
- [3] V. Dunjko and H. J. Briegel, "Machine learning & artificial intelligence in the quantum domain: a review of recent progress," *Reports on Progress in Physics*, vol. 81, no. 7, p. 074001, 2018.
- [4] J. Biamonte, P. Wittek, N. Pancotti, P. Rebentrost, N. Wiebe, and S. Lloyd, "Quantum machine learning," *Nature*, vol. 549, no. 7671, pp. 195-202, 2017.
- [5] M. Schuld, I. Sinayskiy, and F. Petruccione, "An introduction to quantum machine learning," *Contemporary Physics*, vol. 56, no. 2, pp. 172-185, 2015.
- [6] M. Schuld, I. Sinayskiy, and F. Petruccione, "The quest for a quantum neural network," *Quantum Information Processing*, vol. 13, pp. 2567-2586, 2014.
- [7] M. Cerezo *et al.*, "Variational quantum algorithms," *Nature Reviews Physics*, vol. 3, no. 9, pp. 625-644, 2021.
- [8] V. Havlíček *et al.*, "Supervised learning with quantum-enhanced feature spaces," *Nature*, vol. 567, no. 7747, pp. 209-212, 2019.
- [9] E. Farhi and H. Neven, "Classification with quantum neural networks on near term processors," *arXiv preprint arXiv:1802.06002*, 2018.
- [10] J. Romero, J. P. Olson, and A. Aspuru-Guzik, "Quantum autoencoders for efficient compression of quantum data," *Quantum Science and Technology*, vol. 2, no. 4, p. 045001, 2017.
- [11] K. H. Wan, O. Dahlsten, H. Kristjánsson, R. Gardner, and M. Kim, "Quantum generalisation of feedforward neural networks," *npj Quantum information*, vol. 3, no. 1, p. 36, 2017.
- [12] M. Larocca, N. Ju, D. García-Martín, P. J. Coles, and M. Cerezo, "Theory of overparametrization in quantum neural networks," *Nature Computational Science*, vol. 3, no. 6, pp. 542-551, 2023.
- [13] L. Schatzki, A. Arrasmith, P. J. Coles, and M. Cerezo, "Entangled datasets for quantum machine learning," *arXiv preprint arXiv:2109.03400*, 2021.
- [14] M. S. Akter *et al.*, "Case Study-Based Approach of Quantum Machine Learning in Cybersecurity: Quantum Support Vector Machine for Malware Classification and Protection," in *2023 IEEE 47th Annual Computers, Software, and Applications Conference (COMPSAC)*, 2023: IEEE, pp. 1057-1063.
- [15] M. Grossi *et al.*, "Mixed quantum-classical method for fraud detection with quantum feature selection," *IEEE Transactions on Quantum Engineering*, vol. 3, pp. 1-12, 2022.
- [16] M. Singh, C. Dhara, A. Kumar, S. S. Gill, and S. Uhlig, "Quantum artificial intelligence for the science of climate change," in *Artificial Intelligence, Machine Learning and Blockchain in Quantum Satellite, Drone and Network*: CRC Press, 2022, pp. 199-207.
- [17] G. S. M. Silva and E. L. Drogue, "Quantum machine learning for health state diagnosis and prognostics," in *2022 Annual Reliability and Maintainability Symposium (RAMS)*, 2022: IEEE, pp. 1-7.
- [18] D. J. Egger *et al.*, "Quantum computing for finance: State-of-the-art and future prospects," *IEEE Transactions on Quantum Engineering*, vol. 1, pp. 1-24, 2020.
- [19] A. Nammouchi, A. Kassler, and A. Theocharis, "Quantum Machine Learning in Climate Change and Sustainability: A Short," *Quantum*, vol. 1, p. 1, 2023.
- [20] B. Surendiran, K. Dhanasekaran, and A. Tamizhselvi, "A Study on Quantum Machine Learning for Accurate and Efficient Weather Prediction," in *2022 Sixth International Conference on I-SMAC (IoT in Social, Mobile, Analytics and Cloud)(I-SMAC)*, 2022: IEEE, pp. 534-537.
- [21] A. Melnikov, M. Kordzanganeh, A. Alodjants, and R.-K. Lee, "Quantum machine learning: from physics to software engineering," *Advances in Physics: X*, vol. 8, no. 1, p. 2165452, 2023.
- [22] F. Tacchino *et al.*, "Variational learning for quantum artificial neural networks," *IEEE Transactions on Quantum Engineering*, vol. 2, pp. 1-10, 2021.
- [23] J. Pérez-Guijarro, A. Pages-Zamora, and J. R. Fonollosa, "Relation between quantum advantage in supervised learning and quantum computational advantage," *IEEE Transactions on Quantum Engineering*, 2023.
- [24] Z. Abohashima, M. Elhosen, E. H. Houssein, and W. M. Mohamed, "Classification with quantum machine learning: A survey," *arXiv preprint arXiv:2006.12270*, 2020.
- [25] D. K. Park, C. Blank, and F. Petruccione, "The theory of the quantum kernel-based binary classifier," *Physics Letters A*, vol. 384, no. 21, p. 126422, 2020.
- [26] H. Yano, Y. Suzuki, K. M. Itoh, R. Raymond, and N. Yamamoto, "Efficient discrete feature encoding for variational quantum classifier," *IEEE Transactions on Quantum Engineering*, vol. 2, pp. 1-14, 2021.
- [27] W. Li and D.-L. Deng, "Recent advances for quantum classifiers," *Science China Physics, Mechanics & Astronomy*, vol. 65, no. 2, p. 220301, 2022.
- [28] A. Zhang, X. He, and S. Zhao, "Quantum algorithm for neural network enhanced multi-class parallel classification," *arXiv preprint arXiv:2203.04097*, 2022.
- [29] G. Gentinetta, A. Thomsen, D. Sutter, and S. Woerner, "The complexity of quantum support vector machines, 2022. DOI: 10.48550/arXiv:2203.00031," *arXiv preprint ARXIV.2203.00031*.
- [30] M. Russo, E. Giusto, and B. Montrucchio, "Quantum Kernel Estimation With Neutral Atoms For Supervised Classification: A Gate-Based Approach," in *2023 IEEE International Conference on Quantum Computing and Engineering (QCE)*, 2023, vol. 1: IEEE, pp. 219-228.
- [31] Z. Kronic, F. F. Flöther, G. Seegan, N. D. Earnest-Noble, and O. Shehab, "Quantum kernels for real-world predictions based

- on electronic health records," *IEEE Transactions on Quantum Engineering*, vol. 3, pp. 1-11, 2022.
- [32] E. Farhi and S. Gutmann, "Quantum computation and decision trees," *Physical Review A*, vol. 58, no. 2, p. 915, 1998.
- [33] Z. Zhang, Z. Guan, and H. Zhang, "An algorithm of optimization for linear nearest neighbor quantum circuits by parallel processing," in *2018 Eighth International Conference on Instrumentation & Measurement, Computer, Communication and Control (IMCCC)*, 2018: IEEE, pp. 1046-1050.
- [34] N. L. Wach, M. S. Rudolph, F. Jendrzejewski, and S. Schmitt, "Data re-uploading with a single qudit," *Quantum Machine Intelligence*, vol. 5, no. 2, p. 36, 2023.
- [35] O. Lockwood, "An empirical review of optimization techniques for quantum variational circuits," *arXiv preprint arXiv:2202.01389*, 2022.
- [36] X. Lee, X. Yan, N. Xie, Y. Saito, D. Cai, and N. Asai, "Iterative Layerwise Training for Quantum Approximate Optimization Algorithm," *arXiv preprint arXiv:2309.13552*, 2023.
- [37] T. Dutta, A. Pérez-Salinas, J. P. S. Cheng, J. I. Latorre, and M. Mukherjee, "Single-qubit universal classifier implemented on an ion-trap quantum device," *Physical Review A*, vol. 106, no. 1, p. 012411, 2022.
- [38] S. Aminpour, Y. Banad, and S. Sharif, "Quantum Classifier with Iterative Re-Uploading for Universal Classification: Performance Evaluation and Insights," *Bulletin of the American Physical Society*, 2024.
- [39] S. Sharifi and S. Aminpour, "Re-uploading classical data points using Quantum MP Neural Network," in *APS March Meeting Abstracts*, 2023, vol. 2023, p. G00. 289.
- [40] M. Schuld, A. Bocharov, K. M. Svore, and N. Wiebe, "Circuit-centric quantum classifiers," *Physical Review A*, vol. 101, no. 3, p. 032308, 2020.
- [41] Y. LeCun, Y. Bengio, and G. Hinton, "Deep learning," *nature*, vol. 521, no. 7553, pp. 436-444, 2015.
- [42] C. W. Helstrom, "Quantum detection and estimation theory," *Journal of Statistical Physics*, vol. 1, pp. 231-252, 1969.
- [43] M. A. Nielsen and I. L. Chuang, *Quantum computation and quantum information*. Cambridge university press, 2010.
- [44] K. Hornik, "Approximation capabilities of multilayer feedforward networks," *Neural networks*, vol. 4, no. 2, pp. 251-257, 1991.
- [45] D. C. Liu and J. Nocedal, "On the limited memory BFGS method for large scale optimization," *Mathematical programming*, vol. 45, no. 1, pp. 503-528, 1989.
- [46] C. Zhu, R. H. Byrd, P. Lu, and J. Nocedal, "Algorithm 778: L-BFGS-B: Fortran subroutines for large-scale bound-constrained optimization," *ACM Transactions on mathematical software (TOMS)*, vol. 23, no. 4, pp. 550-560, 1997.
- [47] Y. Liu *et al.*, "On centroidal Voronoi tessellation—energy smoothness and fast computation," *ACM Transactions on Graphics (ToG)*, vol. 28, no. 4, pp. 1-17, 2009.
- [48] L. Wang, K. Zhou, Y. Yu, and B. Guo, "Vector solid textures," *ACM Transactions on Graphics (TOG)*, vol. 29, no. 4, pp. 1-8, 2010.
- [49] R. H. Byrd, P. Lu, J. Nocedal, and C. Zhu, "A limited memory algorithm for bound constrained optimization," *SIAM Journal on scientific computing*, vol. 16, no. 5, pp. 1190-1208, 1995.
- [50] P. Virtanen *et al.*, "SciPy 1.0: fundamental algorithms for scientific computing in Python," *Nature methods*, vol. 17, no. 3, pp. 261-272, 2020.
- [51] X. Bonet-Monroig *et al.*, "Performance comparison of optimization methods on variational quantum algorithms," *Physical Review A*, vol. 107, no. 3, p. 032407, 2023.
- [52] A. Pellow-Jarman, I. Sinayskiy, A. Pillay, and F. Petruccione, "A comparison of various classical optimizers for a variational quantum linear solver," *Quantum Information Processing*, vol. 20, no. 6, p. 202, 2021.
- [53] J. A. Nelder and R. Mead, "A simplex method for function minimization," *The computer journal*, vol. 7, no. 4, pp. 308-313, 1965.
- [54] F. Gao and L. Han, "Implementing the Nelder-Mead simplex algorithm with adaptive parameters," *Computational Optimization and Applications*, vol. 51, no. 1, pp. 259-277, 2012.
- [55] S. Abel, A. Blance, and M. Spannowsky, "Quantum optimization of complex systems with a quantum annealer," *Physical Review A*, vol. 106, no. 4, p. 042607, 2022.
- [56] D. Kraft, "A software package for sequential quadratic programming," *Forschungsbericht- Deutsche Forschungs- und Versuchsanstalt für Luft- und Raumfahrt*, 1988.